

---

# An Advanced Aeroelastic Model for Horizontal Axis Wind Turbines

F. Frunzulica<sup>1,2</sup>, H. Dumitrescu<sup>2</sup>, A. Dumitrache<sup>2</sup>, and V. Cardos<sup>2</sup>

<sup>1</sup> “POLITEHNICA” University from Bucharest, Bucharest, Romania  
ffrunzi@aero.pub.ro

<sup>2</sup> “Gheorghe Mihoc – Caius Iacob” Institute of Mathematical Statistics  
and Applied Mathematics, Bucharest, Romania, horia.dumitrescu@ima.ro,  
alexandru.dumitrache@ima.ro, vladimir.cardos@ima.ro

**Summary.** In this paper an advanced aeroelastic numerical tool for horizontal axis wind turbines is presented. The tool is created by non-linear coupling an unsteady aerodynamic model based on the lifting-line approximation with an elastodynamic model based on the beam approximation. The aero-to-elastic interface defines the loads exercised on the structure, whereas the elastic-to-aero interface transmits the rates of deformations. The aeroelastic model is evaluated through comparisons of its predictions with experimental data as well as with predictions obtained by simpler models.

## 1 Introduction

The design problem of horizontal axis wind turbines (HAWT) is related to two dominant model problems: the aerodynamic problem and the elastodynamic one. Their combination leads to the aeroelastic problem of a horizontal axis wind turbine. Input to this problem is the wind inflow conditions.

In this work, the authors present a non-linear advanced aeroelastic model based on a lifting line model as regards the aerodynamics, and a beam structural model adapted to this problem, useful to a number of design problems.

## 2 The Numerical Method

The key point of the approach adopted herein is based on the formulation of the aeroelastic problem as an appropriate coupling of two different problems: the aerodynamic and the elastodynamic.

### 2.1 The Aerodynamic Model

The response of an horizontal axis wind turbine to dynamic excitation is a special case of the aerodynamic performance problem. In this connection, a computational environment based on a lifting line method [2, 3], and a semiempirical dynamic stall model of Leishman and Beddoes [4] has been developed. This method is an unsteady model based on the vorticity filament approximation of the vorticity on blades.

For the classical prescribed wake-lifting line blade model, the unknown quantity is the spanwise bound circulation distribution. The relationship for the section bound circulation ( $\Gamma$ ) can be shown to be related to the local velocity ( $U$ ), section chord ( $c$ ), and section lift coefficient ( $C_L$ ) through the Kutta-Joukowski theorem,

$$\Gamma = \frac{1}{2} c C_L(\alpha) U \tag{1}$$

The local velocity and effective angle of attack ( $\alpha$ ) are functions of the tangential velocity ( $U_T$ ), the local axial and azimuthal induced velocities ( $u, w$ ), wind velocity ( $V_w$ ), and blade pitch angle ( $\theta_p$ ),

$$U = \left[ (U_T + w)^2 + (V_w - u)^2 \right]^{1/2}, \alpha = -\theta_p + \tan^{-1} \left( \frac{V_w - u}{U_T + w} \right), U_T = \Omega r \tag{2}$$

The components of the induced velocity for a given wake geometry, at control point ( $i$ ) and at any time  $k \Delta t$ , can be shown to be a function of the bound circulation distribution and individual vortex filament influence coefficients ( $GC$ ) as

$$u_i^{(k)} = \frac{1}{4\pi R} \sum_{j=1}^N GC_{u,ij}^{(k)} \Gamma_j^{(k)}, w_i^{(k)} = \frac{1}{4\pi R} \sum_{j=1}^N GC_{w,ij}^{(k)} \Gamma_j^{(k)} \tag{3}$$

where  $N$  is the number of blade inflow solution stations [3]. The total lift force coefficient is given by sum of circulatory and noncirculatory components under attached flow conditions

$$C_L^\beta(t) = C_{LI}(t) + C_{LC}(t) \tag{4}$$

and by sum of nonlinear separation and vortex components under dynamic stall conditions [4]

$$C_L^s(t) = C_{LF}(t) + C_{LV}(t) \tag{5}$$

The nonlinear solution is based on the linearization of the relationships given above ((1), (2), (3), and (4) or (5)) to form a system of linear equations which can be corrected for the actual nonlinearities of the problem by a lagged iteration procedure. Since the induced velocities are also functions of the circulation distribution (3), the equation at the  $i$ th blade segment (1) can be reformulated as

$$\Gamma_i = \frac{1}{2} c a \left( U_T \bar{\theta} - \frac{1}{4\pi R} \sum_{j=1}^N G C_{u,ij} \Gamma_j \right) + \frac{1}{2} c a C_{f,i} \tag{6}$$

where  $a$  is the linear lift curve slope,  $\bar{\theta} = -\theta_p - \alpha_0 + V_w/U_T$ ,  $\alpha_0$  is the zero lift offset angle, and  $C_f$  is the correction to the linearized equations for the nonlinearities of the actual problem,

$$C_f = U (C_L/a) - U_T (-\theta_p - \alpha_0 + (V_w - u)/U_T)$$

This equation can be written for each blade segment, and thus, a system of simultaneous linear equations results if the correction term ( $C_f$ ) is assumed known. In matrix form, this can be expressed as

$$[A] [\Gamma^n] = [B] - [C \Gamma^{n-1}] \tag{7}$$

where  $[A]$  is the matrix of influence coefficients and  $[C \Gamma^{n-1}]$  is a correction vector calculated based on the circulation solution from the previous iteration. Once (7) has been solved, the circulation distribution on blades is known at the present time and the foregoing procedure may be repeated to obtain the solution at future times. The last phase of the computations consists of calculations of blade forces and the performance.

### 2.2 The Elastodynamic Model

The aspect ratio of wind turbine blades is, usually large and, therefore, beam theory can be used to describe, the elastodynamic behaviour of the blade. Let  $O [X_e, Y_e, Z_e]$  denote the beam coordinate system, and it is assumed that the elastic axis is straight and coincides with axis  $Y_e$ . In this model three types of deformations are introduced:  $\delta_x(y)$  – the bending deformation along  $X_e$  direction (flapwise bending),  $\delta_z(y)$  – the bending deformation along  $Z_e$  direction (leadwise bending) and  $\theta_y(y)$  – the spanwise torsional deformation.

The first step in structural computation is to calculate beam cross-sectional properties of thin-walled beam, multicell, nonhomogeneous, closed sections, within the framework of Bernoulli’s bending theory and St. Venant torsion theory [5, 7]. The key idea is the approximation of the airfoil’s shape by  $ne$  straight, homogeneous elements. The thickness of every element is considered constant and is evenly distributed across the two sides of its midline.

At the beginning, the element coordinates can be given with respect to any coordinate system, but after the calculation of the elastic centre coordinates, we switch to the elastic coordinate system.

**The finite element technique.** By using Lagrange equations the following linear equations of motion are obtained [1, 8]

$$M \ddot{D}_n + C \dot{D}_n + K D_n = R_n^{ext} \tag{8}$$

where  $M = \rho \int_V N^T N dV$  is the mass matrix,  $C = \int_V N^T C^* N_d dV$  is the structural damping matrix,  $K = \int_V N_d^T E N_d dV$  is the stiffness matrix,  $R^{ext}$  is the load vector,  $D$  is the displacement vector, which contain the degrees of freedom,  $N_d$  – the derivative matrix of shape functions, and  $N$  – the matrix of shape functions (for the beam element the shape functions most commonly used are the third-degree polynomials and the first degree in the case of torsion) [8].

The time advancement of (8) with the appropriate initial conditions is performed with the specialized algorithm (Crank-Nicolson) method [3]. This is an unconditionally stable implicit one-step method, which is second order accurate in time.

### 2.3 Coupling Models

The solution of the aeroelastic problem requires the coupling of an aerodynamic and an elastodynamic model. In previous paragraphs a brief description of each part was done separately. In this paragraph the basic principles of the communication between the two parts will be discussed.

As regards the elastodynamic part, the load vector must be input. This vector is calculated by superimposing the gravitational forces on the aerodynamic loads. The quantities that have to be transferred from the aerodynamic part are, therefore, the aerodynamic forces that act on the blade.

The solution of (8) yields the vector  $D$  of the deformations, the vector  $\dot{D}$  of the deformation rates and the vector  $\ddot{D}$  of the accelerations at the nodes of the beam that simulates the blade.

The main modules can be summarized in the following flowchart Fig. 1.

The flowchart of the aeroelastic code has the following steps: (a) Initialize code; (b) Perform same pure aerodynamic steps for the calculation of the circulation distribution; (c) Time marching scheme. For every time step: (c.1) start time step; (c.2) calculate the circulation distribution; (c.3) calculate the force and the velocity distribution on the blades; (c.4) perform elastodynamic

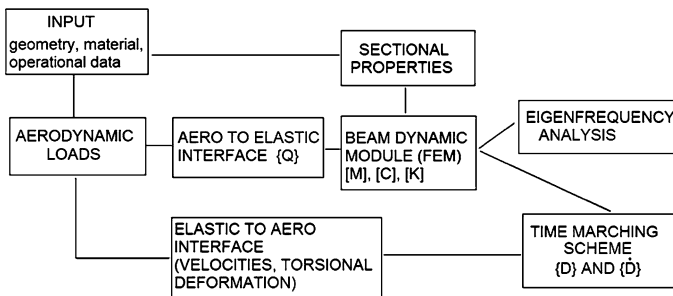


Fig. 1. The flowchart of the coupling between aerodynamic and elastodynamic models

**Table 1.** Comparison between experiment and numerical results

	Case 1		Case 2	
	Experiment	Aeroelastic code	Experiment	Aeroelastic code
$U_\infty$ (m/s)	12.5	12.5	8.7	8.7
$t_{1,st}$ (s)	4.70	14.0	2.0	21.0
$t_{1,end}$ (s)	6.00	15.3	2.5	21.5
$t_{2,st}$ (s)	34.58	24.0	32.0	34.0
$t_{2,end}$ (s)	35.7	25.12	32.7	34.7
$\theta_1$ (deg)	-1.164	-1.164	-0.07	-0.07
$\theta_2$ (deg)	-3.19	-3.19	-3.716	-3.716

steps for a period of time equal to aerodynamic time step; (c.5) circulation calculation step; (c.6) go to next time step. The only communication between the two parts is in step (c.4) where the aerodynamic forces are imposed on the beam and the elastodynamic problem is solved.

### 3 Results

The results presented in the sequel concern the two cases of double pitch steps for the Tjaereborg HAWT, for which experimental data are available [6]. The parameters used for each case are (Table 1) : the inflow velocity  $-U_\infty$ (m/s), the starting time of first pitch step  $t_{1,st}$  (s), the ending time of first pitch step  $t_{1,end}$  (s), the starting time of second pitch step  $t_{2,st}$  (s), the ending time of second pitch step  $t_{2,end}$  (s), the initial pitch angle  $\theta_1$  (deg), the pitch angle after the first pitch step  $\theta_2$  (deg). The numerical results are shown in Fig. 2.

### 4 Conclusions

A complete aeroelastic tool has been presented together with its self consistency tests and some results. In this stage, we cannot conclude on its accuracy. However, the experience suggests that this could be expected.

There are three points that must be underlined: (1) in some tests it appeared necessary to introduce artificial damping; (2) the coupling, within the context of approach described, must be non-linear and (3) the computational effort required to couple the aerodynamics with the structural part, is small compared to the whole.

Prospective work: we will make a most elaborate model based on the coupling of the aerodynamic model with a structural code based on the shell model and composite materials.

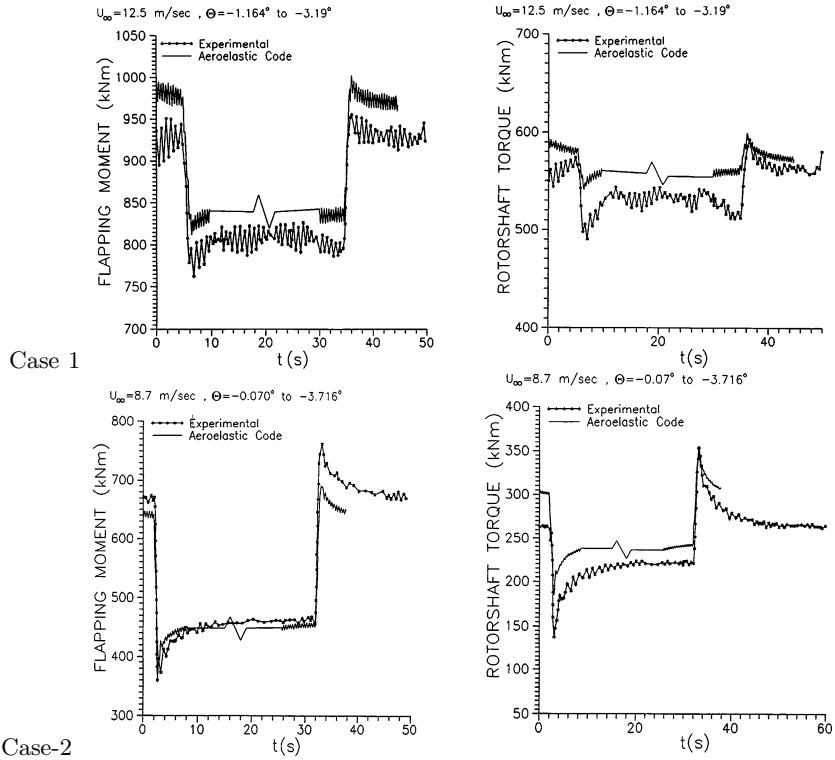


Fig. 2. Comparison between experiment and aeroelastic code

## References

1. Bisplinghoff, R.L., Ashley, H., Halfman, R.: *Aeroelasticity*. Dover, New York (1996)
2. Dumitrescu, H., Cardos, V.: *Int. J. Appl. Mech. Eng.* **9**(4), 675–686 (2004)
3. Dumitrescu, H., Cardos, V., Frunzulica, F., Dumitrache, A.: *Aerodynamics, Aeroelasticity and Aeroacoustics for Wind Turbines*. Romanian Academy, Bucharest, Romania (2007)
4. Leishman, J.G., Beddoes, T.S.: *J. Am. Helicopter Soc.* **34**(3), 3–17 (1989)
5. Megson, T.H.G.: *Aircraft Structures for Engineering Students*. Edward Arnold, London (1977)
6. Oye, S.: *Tjaereborg Wind Turbine: Fifth Dynamic Inflow Measurement*. AFM VK-233, Department of Fluid Mechanics, Technical University of Denmark, Lyngby, Denmark (1992)
7. Timoshenko, S., Goodier, J.N.: *Theory of Elasticity*. McGraw-Hill, New York (1992)
8. Zienkiewics, O.C.: *The Finite Element in Engineering Science*. McGraw-Hill, London (1971)